

ROBUST CONTROL OF CONTACT-RICH ROBOTS VIA NEURAL  
BAYESIAN INFERENCE

by

Nardos Ayele Ashenafi

A dissertation

submitted in partial fulfillment

of the requirements for the degree of

Doctor of Philosophy in Electrical and Computer Engineering

Boise State University

May 2023

© 2023

Nardos Ayele Ashenafi

ALL RIGHTS RESERVED

# CONTENTS

LIST OF FIGURES . . . . .	vii
LIST OF TABLES . . . . .	viii
1 BACKGROUND . . . . .	1
1.1 Contact Modeling with Linear Complementarity Problem . . . . .	1
1.2 Passivity-Based Control (PBC) . . . . .	1
1.2.1 Neural PBC . . . . .	2
1.2.2 Neural Interconnection and Damping Assignment PBC . . . . .	3
1.3 Bayesian Learning . . . . .	4
2 SWITCHING CONTROL WITH DEEP-NET MIXTURE OF EXPERTS . . . . .	8
2.1 Introduction . . . . .	8
2.2 Learning Deep-Net Mixture of Expert Controllers . . . . .	8
2.3 Experimental Results . . . . .	8
2.3.1 Stable Switching Between Unstable Systems . . . . .	8
2.3.2 Cartpole with Wall Contacts . . . . .	8
2.4 Conclusion . . . . .	8
3 UNCERTAINTY HANDLING VIA NEURAL BAYESIAN INFERENCE . . . . .	9
3.1 Introduction . . . . .	9

3.2	Theoretical Justification of Robustness . . . . .	9
3.2.1	Optimal Control under Parameter Uncertainty . . . . .	9
3.2.2	Optimal Control under Parameter Uncertainty and Measurement Noise	12
3.3	Learning Robust Stochastic Controllers . . . . .	15
3.3.1	Bayesian Neural PBC . . . . .	15
3.3.2	Bayesian Neural Interconnection and Damping Assignment PBC . . .	15
3.4	Experimental Results . . . . .	15
3.4.1	Simple Pendulum . . . . .	15
3.4.2	Inertia Wheel Pendulum . . . . .	15
3.4.3	Rimless Wheel . . . . .	15
3.5	Conclusion . . . . .	15
	REFERENCES . . . . .	15
	APPENDICES . . . . .	17

## LIST OF FIGURES

3.1	The optimal control parameter distribution given that the system parameter $p$ is normally distributed with mean $\hat{p} = 5$ and $\sigma_p = 5$ . The red and black arrows respectively indicate the optimal control parameter without considering the randomness of $p$ , and the expected value of the optimal control parameter distribution. . . . .	11
3.2	The optimal controller parameter magnitude $ \theta^* $ . . . . .	14
3.3	The minimal expected cost $\mathbb{E}[\mathcal{J}]$ . . . . .	14

## LIST OF TABLES

# CHAPTER 1: BACKGROUND

## 1.1 Contact Modeling with Linear Complementarity Problem

## 1.2 Passivity-Based Control (PBC)

Let  $x \in \mathcal{X} \subset \mathbb{R}^{2n}$  denote the state of the robot. The state  $x$  is represented in terms of the generalized positions and momenta  $x = (q, p)$ . With  $M$  denoting the symmetric, positive-definite mass matrix, the Hamiltonian  $H$  of the robot is expressed as

$$H(q, p) = \frac{1}{2} p^\top M^{-1}(q) p + V(q), \quad (1.1)$$

where  $V(q)$  represents the potential energy. The system's equations of motion can then be expressed as

$$\begin{bmatrix} \dot{q} \\ \dot{p} \end{bmatrix} = \begin{bmatrix} 0 & I_n \\ -I_n & 0 \end{bmatrix} \begin{bmatrix} \nabla_q H \\ \nabla_p H \end{bmatrix} + \begin{bmatrix} 0 \\ G(q) \end{bmatrix} u, \quad (1.2)$$

$$y = G^\top \dot{q},$$

where  $G(q) \in \mathbb{R}^{n \times m}$  is the input matrix,  $I_n$  denotes the  $n \times n$  identity matrix, and  $u \in \mathbb{R}^m$  is the control input. The system (1.2) is *underactuated* if  $\text{rank } G = m < n$ .

The main idea of passivity-based control (PBC) [1] is to design the input  $u$  with the objective of imposing a desired storage function  $H_d : \mathcal{X} \rightarrow \mathbb{R}$  on the closed-loop system, rendering it passive and consequently stable. In the standard formulation of PBC, the control comprises an energy shaping term and a damping injection term:

$$u = u_{es}(x) + u_{di}(x). \quad (1.3)$$

For mechanical systems, one solution to the PBC problem is of the form

$$\begin{aligned} u_{es}(x) &= -G^\dagger (\nabla_q H_d - \nabla_q H), \\ u_{di}(x) &= -K_v y, \end{aligned}$$

where  $G^\dagger = (G^\top G)^{-1} G^\top$ , and  $K_v \succ 0$  is the damping gain matrix. The choice for  $H_d$  must satisfy

$$G^\perp (\nabla_q H_d - \nabla_q H) = 0, \quad (1.4)$$

where  $G^\perp G = 0$ , and  $H_d$  has a minimum at the desired equilibrium  $x^*$ .

### 1.2.1 Neural PBC

#### CONTINUITY

However, the closed-form solution to the partial differential equations (PDEs) in (1.4) is intractable. The deterministic NEURALPBC framework presented in [2] solves the PDEs



given in (1.4) by rewriting the PBC problem as an optimization problem of the form

$$\begin{aligned}
& \underset{\theta}{\text{minimize}} && \int_0^T \ell(\phi, u^\theta(\phi)) \, dt, \\
& \text{subject to} && \dot{x} = \begin{bmatrix} \nabla_p H \\ -\nabla_q H \end{bmatrix} + \begin{bmatrix} 0 \\ G(q) \end{bmatrix} u^\theta, \\
& && u^\theta = -G^\dagger \nabla_q H_d^\theta - K_v^\theta G^\top \nabla_p H_d^\theta,
\end{aligned} \tag{1.5}$$

where  $T > 0$  is the time horizon,  $\ell : \mathcal{X} \times \mathcal{U} \rightarrow \mathbb{R}$  is a running cost function to be defined, and  $\phi(t; x_0, u^\theta)$  is the flow of the dynamical system. The NEURALPBC technique adds three important features to the classical PBC framework.

1. The optimization problem finds an approximate solution to the PDEs in (1.4).
2. Desired system behavior is explicitly introduced into the optimization via the performance objective  $\ell$ .
3. The universal approximation capabilities of neural networks are leveraged to parameterize the desired Hamiltonian  $H_d^\theta$ .

### 1.2.2 Neural Interconnection and Damping Assignment PBC

IDAPBC, a variant of PBC, selects a particular structure for  $H_d$

$$H_d(q, p) = \frac{1}{2} p^\top M_d^{-1}(q) p + V_d(q), \tag{1.6}$$

such that the control input must satisfy the PDEs given by

$$G^\perp \{ \nabla_q H - M_d M^{-1} \nabla_q H_d + J_2 M_d^{-1} p \} = 0. \tag{1.7}$$

The objective is to learn  $V_d$  and the entries of  $M_d$  and  $J_2$  matrices. Once  $V_d$ ,  $M_d$  and  $J_2$  are obtained, the energy-shaping control and the damping injection term are given by

$$\begin{aligned} u_{es} &= G^\dagger \left( \nabla_q H - M_d M^{-1} \nabla_q H_d + J_2 M_d^{-1} p \right), \\ u_{di} &= -K_v G^\top \nabla_p H_d, \end{aligned} \tag{1.8}$$

respectively, where  $G^\dagger = (G^\top G)^{-1} G^\top$ .

The closed-form solution to the PDEs in (1.7) is intractable. Hence, the deterministic NEURAL-IDAPBC framework introduced in [3] formulates the following optimization problem that finds an approximate solution to the PDEs.

$$\begin{aligned} \underset{\theta}{\text{minimize}} \quad & \|l_{\text{IDA}}(x)\|^2 = \|G^\perp \{ \nabla_q H - M_d M^{-1} \nabla_q H_d + J_2 M_d^{-1} p \} \|^2, \\ \text{subject to} \quad & M_d^\theta = (M_d^\theta)^\top \succ 0, \\ & J_2^\theta = -(J_2^\theta)^\top, \\ & q^* = \underset{q}{\text{argmin}} V_d^\theta. \end{aligned} \tag{1.9}$$

where  $V_d^\theta$  and the entries of the  $M_d^\theta$  and  $J_2^\theta$  matrices are parameterized by neural networks.

### 1.3 Bayesian Learning

The objective of Bayesian learning is to determine a stochastic model (target function) that best fits observed data  $\mathcal{D}$  with inherent noise. Let this stochastic target function be represented by  $F(x; \theta) : \mathcal{X} \rightarrow \mathbb{R}^t$ , where  $\theta \in \Theta \subset \mathcal{R}^v$  is a multivariate random variable that parameterizes the model. Given prior belief on the distribution of the parameters  $p(\theta)$ , Bayesian learning finds a posterior distribution  $p(\theta \mid \mathcal{D})$  over  $\theta$  that maximizes the likelihood of the target function generating the dataset  $\mathcal{D}$  [4]. This can be expressed in terms of Bayes'

theorem as

$$p(\theta|\mathcal{D}) = \frac{p(\mathcal{D} | \theta)p(\theta)}{p(\mathcal{D})} = \frac{p(\mathcal{D} | \theta)p(\theta)}{\int_{\theta} p(\mathcal{D} | \theta')p(\theta')d\theta'}, \quad (1.10)$$

where  $p(\mathcal{D} | \theta)$  is the likelihood function and  $p(\mathcal{D})$  is the evidence. While the likelihood and prior distribution can be expressed explicitly, the evidence is intractable. This calls for techniques that approximate or find the exact posterior distribution, some of which are discussed in the following section.

## Posterior Distribution

Bayesian learning provides various techniques to infer the posterior distribution over the parameters  $\theta$ . Two of the most famous techniques are discussed as follows.

1. Markov Chain Monte Carlo (MCMC) methods: learn the exact posterior distribution by collecting samples of  $\theta$  either through random walk (e.g. Metropolis-Hastings) or following the gradient of the likelihood (e.g. Hamiltonian Monte Carlo). Metropolis-Hastings methods collect samples of  $\theta$  from a conditional probability distribution until the samples converge to an equilibrium distribution per the properties of irreducible and aperiodic Markov chains [5]. Hamiltonian Monte Carlo (HMC) method, shown in detail in Algorithm 1, also finds the equilibrium distribution of the Markov chain, but unlike Metropolis-Hastings, it efficiently searches the parameter space through the gradient of the likelihood. In the case of HMC, the Markov chain is generated from two first-order differential equations shown in lines 5-7 of Algorithm 1. While HMC method learns the exact posterior distribution, it has slow convergence properties for high-dimensional parameters. In such cases, techniques such as variational inference

---

**Algorithm 1** Hamiltonian Monte Carlo

---

- 1: Select initial state  $\theta$  and momentum  $r$  from prior knowledge
  - 2: Select regularization coefficient  $\lambda$
  - 3: Create a set  $\Theta$  to collect samples of  $\theta$
  - 4: Define  $p(\theta, \mathcal{D}) \propto \exp(-E(\theta, \mathcal{D}))$ ,  $E(\theta, \mathcal{D}) = \sum_{d \in \mathcal{D}} \|F(x; \theta) - d\|^2 + \lambda \|\theta\|^2$
  - 5: **for**  $t = 0 : \Delta t : T$  **do**
  - 6:      $r(t + \Delta t/2) = r(t) - \frac{\Delta t}{2} \frac{\partial E}{\partial \theta_i}(\theta(t), \mathcal{D})$
  - 7:      $\theta(t + \Delta t) = \theta(t) + \Delta t r(t + \Delta t/2)$
  - 8:      $r(t + \Delta t) = r(t + \Delta t/2) - \frac{\Delta t}{2} \frac{\partial E}{\partial \theta_i}(\theta(t + \Delta t), \mathcal{D})$
  - 9:      $\nu \sim \text{Uniform}[0, 1]$
  - 10:    **if**  $E(\theta(t + \Delta t), \mathcal{D}) < E(\theta(t), \mathcal{D})$  **then**
  - 11:        $\Theta \leftarrow \Theta \cup \theta(t + \Delta t)$
  - 12:    **else if**  $\nu < \exp(E(\theta(t), \mathcal{D}) - E(\theta(t + \Delta t), \mathcal{D}))$  **then**
  - 13:        $\Theta \leftarrow \Theta \cup \theta(t + \Delta t)$
  - 14:    **else if**  $\nu > \exp(E(\theta(t), \mathcal{D}) - E(\theta(t + \Delta t), \mathcal{D}))$  **then**
  - 15:       Reject  $\theta(t + \Delta t)$
  - 16: **Return**  $\Theta$
- 

compromise accuracy of the posterior distribution for speed of convergence.

2. Variational Inference (VI): this technique selects a posterior distribution  $q(\theta; z)$  from the conjugate families of the likelihood and prior distributions. The goal is to learn the distribution parameters  $z$  that minimize the Kullback-Leibler divergence or equivalently maximize the evidence lower bound (ELBO). The ELBO,  $\mathcal{L}$ , is given by [6]

$$\begin{aligned} \mathcal{L}(\mathcal{D}, z) &= \mathbb{E}_{\theta \sim q} [\log(p(\theta, \mathcal{D}; z)) - \log(q(\theta; z))] , \\ p(\theta, \mathcal{D}; z) &= p(\mathcal{D} \mid \theta; z)p(\theta), \end{aligned} \tag{1.11}$$

where  $p(\mathcal{D} \mid \theta; z)$  is the likelihood function.

**Remark 1.** *For continuous posterior distribution, the ELBO given in equation (1.11) is redefined using differential entropy, which expresses the prior and posterior in terms of their probability density functions. In this case, the likelihood  $p(\theta \mid \mathcal{D}; z)$  is also a probability density function and the ELBO is not bounded by zero.*

The power of Bayesian learning lies in its ability to build a target function and make predictions that integrate over uncertainties [7]. These predictions can be found by marginalizing the model over the posterior as follows [8].

$$\hat{F}(x) = \frac{1}{N} \sum_{\theta \sim q} F(x, \theta), \quad (1.12)$$

where  $N$  is the number of samples drawn from the posterior. Moreover, Bayesian frameworks can quantify the confidence in the predictions through the variance of the predictive distribution,  $p(F \mid x, \mathcal{D})$ . The variance of  $p(F \mid x, \mathcal{D})$  is given by [8]

$$\Sigma_{F \mid x, \mathcal{D}} = \frac{1}{N-1} \sum_{\theta \sim q} \left\| F(x, \theta) - \frac{1}{N} \sum_{\theta \sim q} F(x, \theta) \right\|^2. \quad (1.13)$$

## **CHAPTER 2:**

# **SWITCHING CONTROL WITH DEEP-NET MIXTURE OF EXPERTS**

### **2.1 Introduction**

### **2.2 Learning Deep-Net Mixture of Expert Controllers**

### **2.3 Experimental Results**

#### **2.3.1 Stable Switching Between Unstable Systems**

#### **2.3.2 Cartpole with Wall Contacts**

### **2.4 Conclusion**

# CHAPTER 3:

## UNCERTAINTY HANDLING VIA NEURAL BAYESIAN INFERENCE

### 3.1 Introduction

### 3.2 Theoretical Justification of Robustness

In this section, we demonstrate the improved robustness properties of Bayesian learning over point-estimates of a policy. This theoretical justification is given by a toy example, where closed-form calculation of the point-estimates and posterior distributions for the optimal controller is provided.

#### 3.2.1 Optimal Control under Parameter Uncertainty

Let us consider the first-order scalar control system, whose system parameter  $p$  is uncertain:

$$\begin{cases} \dot{x} = px + u, & x(0) = x_0 \\ u(x) = \theta x. \end{cases} \quad (3.1)$$

We assume that  $p \sim \mathcal{N}(\hat{p}, \sigma_p^2)$  where  $\hat{p}$  designates our best prior point estimate of the system parameter  $p$  and  $\sigma_p > 0$  quantifies the uncertainty in the knowledge of the system parameter. The controller is set to be linear in the state  $x \in \mathbb{R}$  with its only parameter

$\theta \in \mathbb{R}$  to be determined through optimization. Without loss of generality, we will take the initial condition  $x_0 = 1$ . The performance index to be optimized for determining the best control parameter  $\theta$  is

$$\mathcal{J} = \int_0^T \left( \frac{1}{2} q x^2 + \frac{1}{2} r u^2 \right) dt, \quad (3.2)$$

where  $T$  is the control horizon and  $q \geq 0$  and  $r > 0$  are design parameters. We solve the control system (3.1) to find  $x(t) = e^{(p+\theta)t}$  and plug this into the performance index (3.2) along with the form selected for the controller. Performing the integration over time and letting  $T \rightarrow \infty$ , assuming that  $p + \theta < 0$  then yields the infinite-horizon optimal cost functional

$$\mathcal{J}_\infty = -\frac{1}{4} \frac{q + r\theta^2}{p + \theta}. \quad (3.3)$$

The optimal control parameter  $\theta$  may be found as the appropriate root of  $\nabla_\theta \mathcal{J}_\infty$ .

$$\begin{aligned} \nabla_\theta \mathcal{J}_\infty &= -\frac{r}{4} \frac{(p + \theta)^2 - (p^2 + q/r)}{(p + \theta)^2} = 0, \\ \therefore \theta^* &= g(p) := -p - \sqrt{p^2 + q/r}, \\ g^{-1}(\theta) &= \frac{q}{2r\theta} - \frac{\theta}{2}. \end{aligned} \quad (3.4)$$

The fact that  $p \sim \mathcal{N}(\hat{p}, \sigma_p^2)$  implies that the optimal control parameter has the probability density function

$$\begin{aligned} f_{\theta^*}(\theta^*) &= f_p(g^{-1}(\theta^*)) \left| \frac{d}{d\theta} g^{-1}(\theta^*) \right| \\ &= \frac{1}{\sigma_p \sqrt{2\pi}} \left( \frac{1}{2} \left( 1 + \frac{q}{r\theta^{*2}} \right) \right) \exp \left\{ -\frac{1}{2\sigma_p^2} \left( \frac{q}{2r\theta^*} - \frac{\theta^*}{2} - \hat{p} \right)^2 \right\}, \end{aligned}$$

where  $f_p$  is the Gaussian probability density function with mean  $\hat{p}$  and variance  $\sigma_p^2$ .



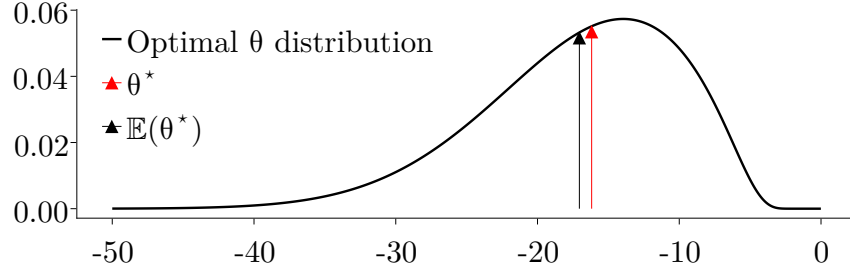


**Figure 3.1:** The optimal control parameter distribution given that the system parameter  $p$  is normally distributed with mean  $\hat{p} = 5$  and  $\sigma_p = 5$ . The red and black arrows respectively indicate the optimal control parameter without considering the randomness of  $p$ , and the expected value of the optimal control parameter distribution.

We can further eliminate the control parameter from the expression for the optimal cost function  $\mathcal{J}_\infty$  by substituting for  $\theta$  from equation (3.4), yielding

$$\begin{aligned}\mathcal{J}^* = h(p) &:= \frac{r}{2} \left( p + \sqrt{p^2 + q/r} \right), \\ h^{-1}(\mathcal{J}^*) &= \frac{\mathcal{J}^*}{r} - \frac{q}{4\mathcal{J}^*}.\end{aligned}$$

Hence, the distribution of the optimal cost conditioned on the system parameter  $p$  is

$$\begin{aligned}f_{\mathcal{J}^*}(\mathcal{J}^*) &= f_p(h^{-1}(\mathcal{J}^*)) \left| \frac{d}{d\theta} h^{-1}(\mathcal{J}^*) \right| \\ &= \frac{1}{\sigma_p \sqrt{2\pi}} \left( \frac{1}{r} + \frac{q}{4\mathcal{J}^{*2}} \right) \exp \left\{ -\frac{1}{2\sigma_p^2} \left( \frac{\mathcal{J}^*}{r} - \frac{q}{4\mathcal{J}^*} - \hat{p} \right)^2 \right\}.\end{aligned}$$

Notice that the distribution of both the optimal control parameter and the optimal cost are elements of the exponential family that are not Gaussian.

There are several advantages of employing Bayesian learning to find the optimal control parameter  $\theta$  as the toy example in this subsection supports. In order to derive some

quantitative results, let us assign some numerical values to the parameters that define the optimal cost function  $(q, r) = (100, 1)$ , our best guess  $\hat{p} = 5$  of the system parameter  $p$  and its standard deviation  $\sigma_p = 5$ .

The optimal control parameter and cost derived for this system whose model is assumed to be known perfectly are given by  $\hat{\theta}^* = -16.180$  with the corresponding estimated cost  $\hat{\mathcal{J}}^* = 8.090$ . This deterministic performance estimate turns out to be *overconfident* when uncertainties in the system parameter are present. For example, if the prior knowledge on the distribution of the system parameter  $p$  is utilized, the expected value of the controller parameter is found as  $\mathbb{E}[\theta^*] = -17.046$  and the corresponding expected cost is  $\mathbb{E}[\mathcal{J}] = 8.523$ . The controller from the deterministic training/optimization is not only overconfident about its performance; but also is less robust against modeling errors, as the Bayesian learning yields a closed-loop stable system for a wider range of values of  $p$ .

Finally, Figure 3.1 shows the optimal control parameter distribution given that the system parameter  $p$  is normally distributed with mean  $\hat{p} = 5$ , standard deviation  $\sigma_p = 5$ . This figure also shows the mean values of the optimal control distribution with the black arrow and the optimal control parameter a deterministic approach would yield in red. We notice that the Bayesian learning that yields the optimal control parameter distribution is more concerned about system stability due to the uncertainty in the parameter  $p$ , a feat that the deterministic training may not reason about.

### 3.2.2 Optimal Control under Parameter Uncertainty and Measurement Noise

Consider the scenario in which the system (3.1) is also subject to measurement errors; that is, our measurement model for the state  $x$  is probabilistic and is distributed according to the Gaussian  $\mathcal{N}(x, \sigma^2)$ . Since the controller uses this measurement to determine its action,

the closed-loop system has to be modelled as a stochastic differential equation (SDE), given by

$$\begin{cases} dx(t) = (p + \theta)x(t) dt + \theta\sigma dW_t, \\ x(0) = 1, \end{cases} \quad (3.5)$$

where  $W$  denotes the Wiener process [9]. The initial state is assumed deterministic and is set to unity for simplicity. The unique solution to this SDE is given by

$$x(t) = e^{(p+\theta)t} + \theta\sigma \int_0^t e^{(p+\theta)(t-s)} dW_s. \quad (3.6)$$

**Lemma 1.** *The conditional expectation  $\mathbb{E}[\mathcal{J} \mid p]$  of the performance index (3.2) given the system parameter  $p$  is*

$$\mathbb{E}[\mathcal{J} \mid p] = -\frac{1}{4} \frac{q + r\theta^2}{p + \theta} \left[ \theta^2 \sigma^2 T + (1 - e^{2T(p+\theta)}) \left( 1 + \frac{1}{2} \frac{\theta^2 \sigma^2}{p + \theta} \right) \right].$$

*Proof.* The proof may be found in the appendix. □

It is easily shown that this quantity is positive for all  $T > 0$ . Furthermore, it blows up as the horizon  $T$  is extended to infinity. This is not surprising since a nonzero measurement noise causes the state to oscillate around the origin, rather than asymptotically converging to it, incurring nonzero cost all the while.

We have kept the system parameter  $p$  constant in this analysis so far. Uncertainty over this variable can be incorporated by taking a further expectation

$$\mathbb{E}[\mathcal{J}] := \mathbb{E}_p [\mathbb{E}_W [\mathcal{J} \mid p]],$$

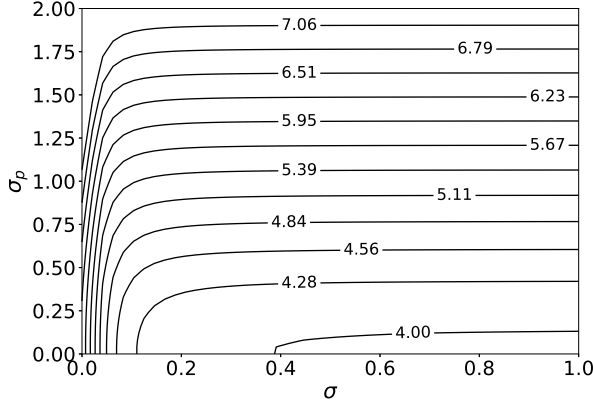


**Figure 3.2:** The optimal controller parameter magnitude  $|\theta^*|$ .

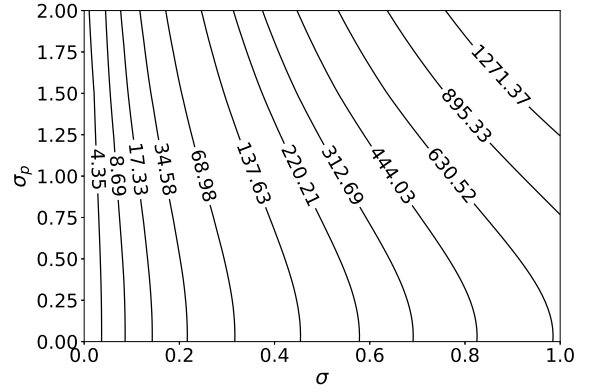


**Figure 3.3:** The minimal expected cost  $\mathbb{E}[\mathcal{J}]$ .

of  $\mathbb{E}_W[\mathcal{J} \mid p]$  over  $p$ , which must be accomplished numerically as it does not admit a closed-form expression.

We can then minimize  $\mathbb{E}[\mathcal{J}]$  over the control parameter in order to study the effects of both kinds of uncertainties on the optimal controller. Such a study is provided in Figures 3.2 and 3.3, where we have plotted the optimal control parameter  $\theta^*$  and the minimal expected cost  $\mathbb{E}[\mathcal{J}]$  as a function of the standard deviations of the measurement noise  $\sigma$  and the system parameter  $\sigma_p$ . The constants we used to generate the data are given by  $q = r = 1$  and  $T = \hat{p} = 3$ . Our first observation is that the magnitude of the optimal control parameter is an increasing function of system parameter uncertainty and a decreasing function of measurement uncertainty. Our second observation is that if the measurement noise is small, then the optimal control parameter is insensitive to system parameter uncertainty as long as this uncertainty is small. The optimal cost shares this insensitivity for an even wider range of values of  $\sigma_p$ . In a similar vein, if the uncertainty in the system parameter is large, then the optimal control parameter is insensitive to the magnitude of the measurement noise. However, the optimal cost is still sensitive to this quantity.

### **3.3 Learning Robust Stochastic Controllers**

#### **3.3.1 Bayesian Neural PBC**

#### **3.3.2 Bayesian Neural Interconnection and Damping Assignment PBC**

### **3.4 Experimental Results**

#### **3.4.1 Simple Pendulum**

#### **3.4.2 Inertia Wheel Pendulum**

#### **3.4.3 Rimless Wheel**

### **3.5 Conclusion**

## BIBLIOGRAPHY

- [1] A. Van Der Schaft, *L2-gain and passivity techniques in nonlinear control*. Springer, 2000, vol. 2.
- [2] N. A. Ashenafi, W. Sirichotiyakul, and A. C. Satici, “Robust passivity-based control of underactuated systems via neural approximators and bayesian inference,” in *2022 IEEE Conference on Decision and Control (under review)*, 2022.
- [3] W. Sirichotiyakul, N. A. Ashenafi, and A. C. Satici, “Robust interconnection and damping assignment passivity-based control via neural bayesian inference,” in *2022 IEEE Transactions on Automatic Control (under review)*, 2022.
- [4] C. M. Bishop, “Pattern recognition,” *Machine learning*, vol. 128, no. 9, 2006.
- [5] W. R. Gilks, S. Richardson, and D. Spiegelhalter, *Markov chain Monte Carlo in practice*. CRC press, 1995.
- [6] S. Cohen, “Bayesian analysis in natural language processing,” *Synthesis Lectures on Human Language Technologies*, vol. 9, no. 2, pp. 1–274, 2016.
- [7] M. E. Tipping, “Bayesian inference: An introduction to principles and practice in machine learning,” in *Summer School on Machine Learning*. Springer, 2003, pp. 41–62.

- [8] L. V. Jospin, W. Buntine, F. Boussaid, H. Laga, and M. Bennamoun, “Hands-on bayesian neural networks—a tutorial for deep learning users,” *arXiv preprint arXiv:2007.06823*, 2020.
- [9] L. C. Evans, *An introduction to stochastic differential equations*. American Mathematical Soc., 2012, vol. 82.

## APPENDIX

### Expectation of the performance index

*Proof of Lemma 1.* Substituting the solution (3.6) of the SDE (3.5) expression into the performance measure (3.2) yields

$$\begin{aligned} \mathcal{J} = & -\frac{1}{4} \frac{q + r\theta^2}{p + \theta} (1 + e^{2T(p+\theta)}) + (q + r\theta^2)\theta\sigma \int_0^T e^{(p+\theta)t} \int_0^t e^{(p+\theta)(t-s)} dW_s dt + \\ & \frac{1}{2}(q + r\theta^2)\theta^2\sigma^2 \int_0^T \left( \int_0^t e^{(p+\theta)(t-s)} dW_s \right)^2 dt \end{aligned}$$

The conditional expectation of this quantity given the system parameter  $p$  under the distribution induced by the Wiener process may be computed in closed-form using Itô calculus:

$$\begin{aligned} \mathbb{E}_W [\mathcal{J} \mid p] = & -\frac{1}{4} \frac{q + r\theta^2}{p + \theta} (1 - e^{2T(p+\theta)}) + (q + r\theta^2)\theta\sigma \int_0^T e^{(p+\theta)t} \mathbb{E}_W \left[ \int_0^t e^{(p+\theta)(t-s)} dW_s \mid p \right] dt + \\ & \frac{1}{2}(q + r\theta^2)\theta^2\sigma^2 \int_0^T \mathbb{E}_W \left[ \left( \int_0^t e^{(p+\theta)(t-s)} dW_s \right)^2 \mid p \right] dt \\ = & -\frac{1}{4} \frac{q + r\theta^2}{p + \theta} (1 - e^{2T(p+\theta)}) + \frac{1}{2}(q + r\theta^2)\theta^2\sigma^2 \int_0^T \left( \int_0^t e^{2(p+\theta)(t-s)} ds \right) dt \\ = & -\frac{1}{4} \frac{q + r\theta^2}{p + \theta} (1 - e^{2T(p+\theta)}) + \frac{1}{2}(q + r\theta^2)\theta^2\sigma^2 \int_0^T -\frac{1}{2(p+\theta)} (1 - e^{2T(p+\theta)}) dt \\ = & -\frac{1}{4} \frac{q + r\theta^2}{p + \theta} \left[ \theta^2\sigma^2 T + (1 - e^{2T(p+\theta)}) \left( 1 + \frac{1}{2} \frac{\theta^2\sigma^2}{p + \theta} \right) \right]. \end{aligned}$$

□